Dopant Imaging of Power Semiconductor Device Cross Sections

U. Gysin [a], E. Meyer [a], T. Glatzel [a], Gino Günzburger [b], H. R. Rossmann,[c], T. A. Jung [a,c], S. Reshanov [d], A. Schöner [d], H. Bartolf [e]

[a] Department of Physics, University of Basel, 4056 Basel, Switzerland
[b] Helmholtz-Zentrum Berlin, Hahn-Meitner-Platz 1, 14109 Berlin, Germany
[c] Laboratory for Micro- and Nanotechnology, Paul Scherrer Institute, CH-5232 Villigen PSI, Switzerland
[d] Ascatron AB, Elektrum 207, SE-16440 Kista, Sweden
[e] ABB Switzerland Ltd, Corporate Research, 5405 Baden-Dättwil, Switzerland

e-mail: ernst.meyer@unibas.ch
Keywords: Dopant Imaging, Scanning Probe Microscopy (SPM), Power Semiconductor Devices, Silicon Carbide

1. Introduction

The characterization of power electronic device cross-sections is an essential part of the manufacturing and optimization processes. One of the most important information is the mapping of the utilized dopant concentrations, since they determine the electronic performance of the device. It is found that secondary ion mass spectroscopy (SIMS) is difficult to be applied in case of power semiconductor devices because of the low dopant concentrations (as low as 10^{14} cm^{-3}) and narrow dimensions in the µm range. In this contribution, a dedicated scanning probe microscope [1], operated under ultra-high vacuum conditions, is applied for this purpose. An image of the scanning probe microscope (SPM) instrument is shown in Fig. 1. The most important operation modes are scanning spreading resistance microscopy (SSRM), Kelvin probe force microscopy (KPFM) and scanning capacitance force microscopy (SCFM). On the one hand, SSRM is found to be a robust method. This SPM technique measures the local spreading resistance at relatively high loading forces. The main disadvantage is the destructive nature of this imaging mode, where high normal forces of about 50 µN are required to penetrate through the native oxide layer of the semiconductor surface. On the other hand, KPFM and SCFM are non-contact methods, which are sensitive enough to observe dopant concentrations in the range of 10^{14} to 10^{18} cm^{-3}. KPFM is found to be influenced by surface defects [1], which can lead to partial pinning of the Fermi level and subsequently a reduced contact potential difference (CPD) is observed. The band bending due to defects can be reduced by suitable sub-bandgap illumination of the tip-surface interface.

2, Experimental Results

To demonstrate the capability of our instrument, we performed dopant imaging on Si-based high-voltage super-junction device structures [2]. These structures were manufactured by a demanding and complex trench-etching followed by epitaxial refill process. The trenches have a depth of 60µm, a width of 3µm and are hole-doped by Boron with concentrations in the range of $10^{14}cm^{-3}$. We found [3] that SSRM provides valuable quantitative information about the doping level by comparison of the measured data at the region of interest to previously calibrated epitaxially grown layers. Furthermore, the trenches were investigated by the non-contact method, KPFM, as shown in Fig. 1. KPFM measures the contrast in the CPD signal by applying a bias voltage V_{CPD} to compensate for electrostatic forces, which is very sensitive to defect structures at the surface. A decrease of the defect density by suitable

sample preparation and the reduction of the surface band bending by illumination with sub-bandgap irradiation are feasible strategies to minimize band bending and to optimize the CPD contrast mechanism [4]. SCFM seems to be a valuable method, but still needs further sophisticated modelling to obtain quantitative results. Fig. 2 shows the depletion zone below the probing tip, which leads to the change of the capacitance as a function of dopant density. The radius of curvature of the probing tips is 50nm as shown in the corresponding SEM pictures. In addition, SiC-device structures were investigated with the above mentioned methods. In this case, SSRM was found to be difficult to be applied because of the extreme hardness of SiC (close to diamond), which makes it difficult to form a stable electronic contact between the diamond-coated tip and the SiC surface.

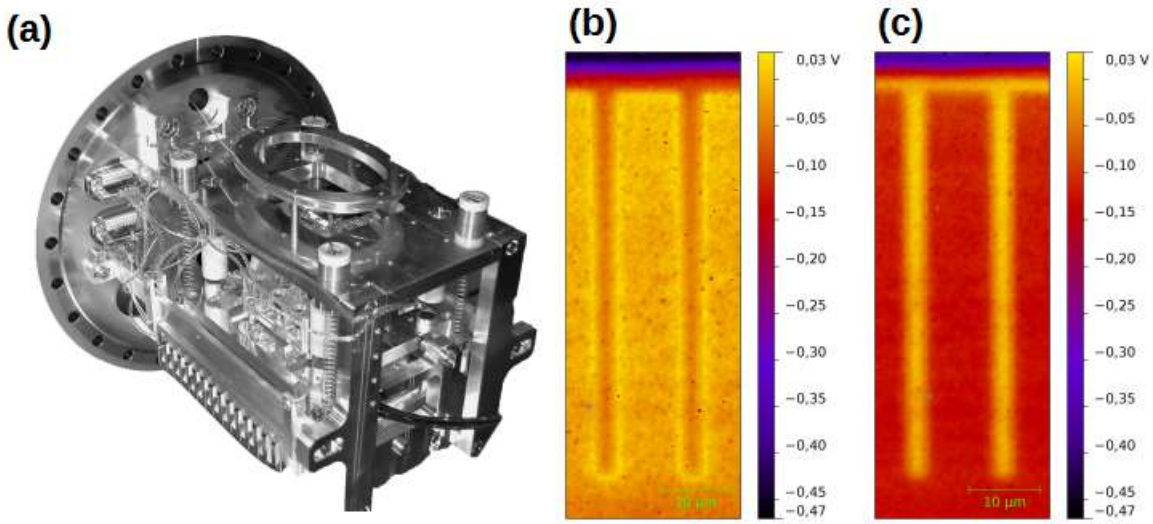

Figure 1: (a) AFM with a 100x100 µm² closed loop scanner operating in UHV conditions with full optical access. Coarse positioning in combination to the added functionality of an optical access provides a nanometer precise access to the regions of interest. KPFM images of a silicon test structure (b) without and (c) with irradiation by sub-bandgap photons. In the upper part, three p- calibrations layers with concentrations of 10^{17},10^{16} and 7 10^{14}cm^{-3} are visible. Below, p-doped trenches with approximate concentrations of 5-7 10^{14}cm^{-3} are surrounded by the n-type substrate.

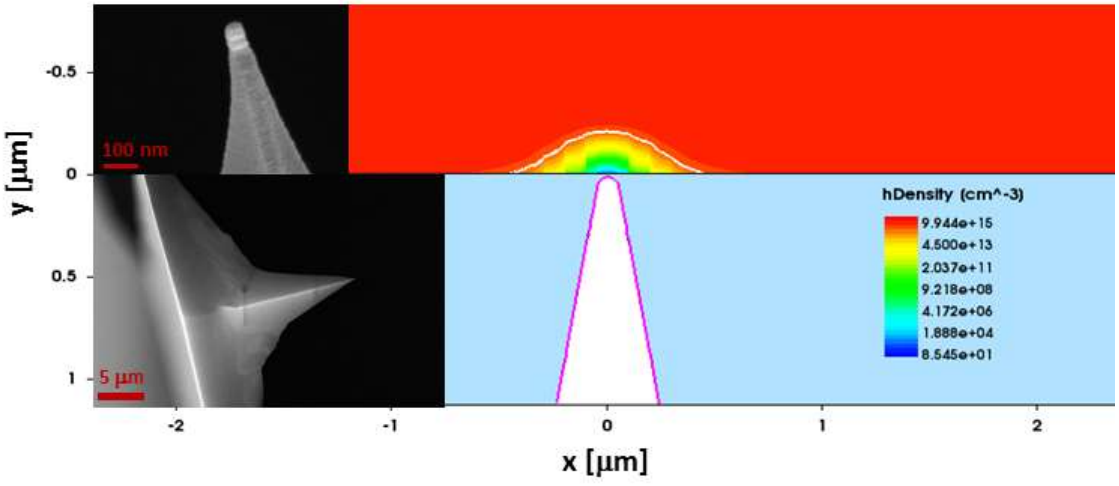

Figure 2: Right side: Synopsys Sentaurus TCAD simulation of the hole density in the vicinity of the probing tip on a silicon surface. The bulk density is p=10^{16}cm^{-3}. The depleted zone at an applied voltage of 5.8V extends

about 200nm into the semiconductor resulting in a measurable capacitance by the SCFM approach. Left side: SEM images of an AFM tip for KPFM and SCFM measurements. The upper, left image exhibits the radius of curvations of approximately 50nm.

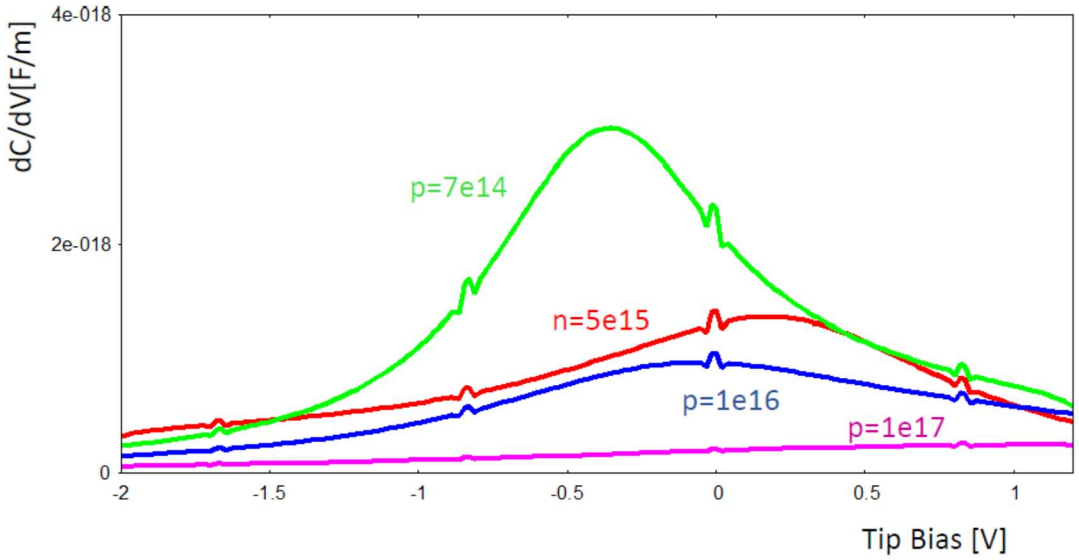

Figure 3: Calculated capacitance gradient for a 50nm tip at 10nm separation above a silicon surface. Interestingly, the biggest gradient is observed for the smallest dopant density which makes SCFM an ideal candidate for dopant imaging with high sensitivity in the low-doping range which is difficult to access by conventional methods (e.g., SIMS).

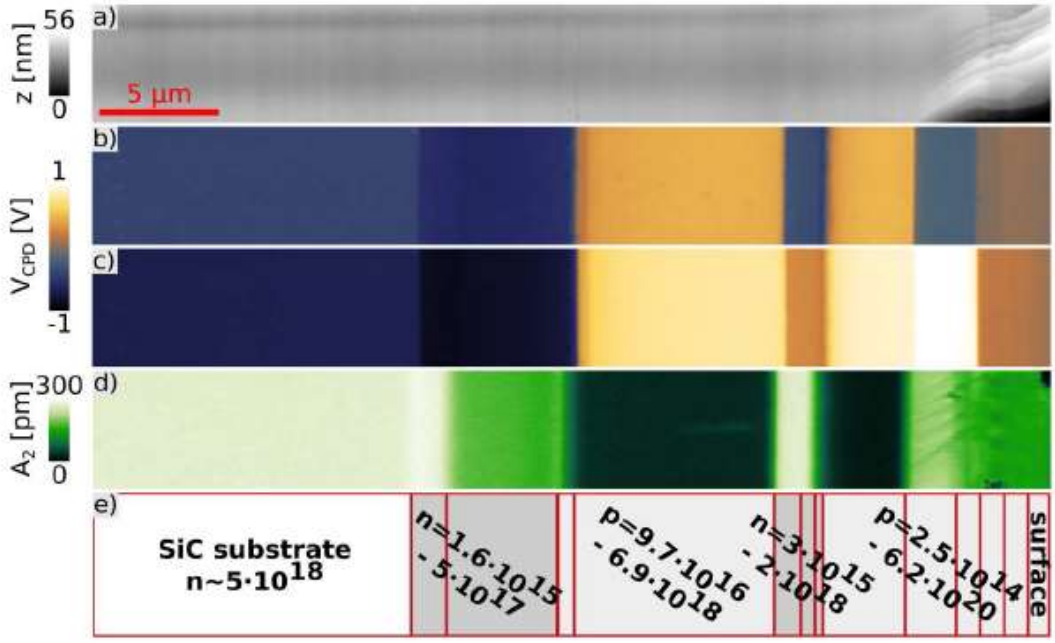

Figure 4. (a) Topography (b) KPFM in dark (c) KPFM with laser irradiation (about 10mW, λ=450-500nm) and (d) SCFM on SiC calibration layers. Bright contrast in SCFM corresponds to the weakest dopant concentrations of $10^{15}cm^{-3}$.

2.1. KPFM Method

Kelvin probe force microscopy (KPFM) relies on the measurement of electrostatic forces between probing tip and sample as a function of applied voltage V_{CPD}[1]. For compensated contact potential, the electrostatic force is at its minimum. Ideally, the local contact potential differences (CPD) are due to the shift of the Fermi energy,

$$CPD = \frac{1}{q}\left(\chi + \frac{E_g}{2} + k_B T \cdot l\,\mathrm{n}\left(\frac{N_A}{n_i}\right) - \phi_m\right) \; CPD = \frac{1}{q}\left(\chi + \frac{E_g}{2} + k_B T \cdot l\,\mathrm{n}\left(\frac{N_A}{n_i}\right) - \phi_m\right)$$

for *p*- doping and

$$CPD = \frac{1}{q}\left(\chi + \frac{E_g}{2} - k_B T \cdot \ln\left(\frac{N_D}{n_i}\right) - \phi_m\right) \; CPD = \frac{1}{q}\left(\chi + \frac{E_g}{2} - k_B T \cdot \ln\left(\frac{N_D}{n_i}\right) - \phi_m\right)$$

for *n*-doping, where χ is the electron affinity, E_g is the band gap, k_B is the Boltzmann constant, T the temperature, q the elementary charge, n_i the intrinsic carrier density, ϕ_m the work function of the metallic tip and N_D is the donor density and N_A the acceptor density. However, the Fermi level can be influenced by interface trap states or surface defects, which leads to band bending and a reduction of the CPD. In extreme cases, the Fermi level is pinned and the CPD would be independent of dopant concentration. The application of sub-band gap irradiation reduces band bending. This results in CPD values which are closer to the theoretical expectations. As shown in Fig. 1 the contrast between *n*- and *p*-doped regions can be inverted (large CPD on *n*-doped areas and smaller CPD on *p*-doped area). Application of light irradiations yields the non-inverted contrast due to the reduction of band bending.

2.2. SCFM Method

Scanning capacitance force microscopy (SCFM) uses force detection to probe the local capacitance. In contrast to scanning capacitance microscopy (SCM), which measures local capacitances by electrical means, SCFM is based on purely mechanical detection by measuring amplitude and phase of the second resonance frequency of the cantilever. Typically, resonance frequencies of the order of 1MHz are used, which means that the method is based on the fast response of the capacitance. It is well known from MIS-capacitance measurements, that the AC-capacitance gives only changes due to accumulation and weak depletion. However, inversion is not observable due to the finite time response of the minority carriers. Similarly, we do observe signals due to accumulation and depletion, where the change of the capacitance due to the depletion capacitance gives the largest signal. As shown in Fig. 3, the strongest signal is observed on the areas with lowly doped concentrations, where the depletion boundary locally penetrates deepest into the semiconductor and the depletion capacitance is smallest, giving rise to large changes of the total capacitance. Simulations with Synopsys Sentaurus TCAD, taking into account the realistic geometry of the cantilever and probing tip (radius of curvature 50 nm and opening angle of 10°), show reasonable agreement between the SCFM measurements on silicon layers. The small ripples of the curves are due to numerical artefacts. Clearly, the largest amplitude is observed for the lowest dopant concentration of $7 \cdot 10^{14}\mathrm{cm}^{-2}$. Subsequently, smaller signals are measured for $1 \cdot 10^{15}$ and $1 \cdot 10^{17}$. SCFM results in a relatively weak contrast for highly doped regions, because the total capacitance is not varying as much during the transition through the depletion region. The contrast on the *n*-region is mirrored at the *y*-axis, but shows similar trends with largest contrast on the lowly doped areas. A comparison between KPFM and SCFM on cross sections of SiC calibration layers shows dopant dependent contrasts, where concentrations between 10^{15} and $10^{20}\mathrm{cm}^{-3}$ can be distinguished, cf. Fig. 4. The amplitude A_2 is related to the voltage derivative of the force gradient (cf. Fig. 3)

3. Conclusion

Dopant imaging of cross-sections of semiconductor power devices has been successfully demonstrated for silicon and silicon carbide devices. In the case of silicon, SSRM is found to be a reliable technique, which is based upon the application of relatively large normal forces of about 50 μN, which generate an ohmic-like contact between SPM tip and sample during the scan. In the case of silicon carbide, SSRM is difficult to be applied because of the hardness of SiC, which is quite close to diamond. In this case, the non-contact methods KPFM and SCFM provide useful information, but are significantly affected by defect states [1]. Sub-band gap irradiation reduces band bending and provides more reliable CPD contrast. SCFM gives the strongest contrast on the regions with lowest dopant concentrations. There, the reduction of the total capacitance due to the large depletion layer is the strongest.

Acknowledgements

This work was supported in part by the Swiss National Science Foundation and the Nano Argovia program of the Swiss Nanoscience Institute.

References

[1] Project A1109 WGB-NPA, Industry Partner: H. Bartolf, PI: E. Meyer, refer to SNI Annual Report (2013).
U. Gysin, T. Glatzel, T. Schmölzer, H. Bartolf, A. Schöner, S. Reshanov and E. Meyer, "Large Area Scanning Probe Microscope in Ultra-High Vacuum Demonstrated for Electrostatic Force Measurements", submitted to Beilstein Journal of Nanotechnology (2015)

[2] H. Bartolf, A. Mihaila, I. Nistor, M. Jurisch, B. Leibold, M. Zimmermann, "Development of a 60μm Deep Trench and Refill Process for Manufacturing Si-Based High-Voltage Super-Junction Structures,"IEEE Transactions On Semiconductor Manufacturing, vol. 26, no. 4, pp. 529-541, 2013.

[3] H. Bartolf et al, *Proc. ISPSD 2015*, Hong-Kong, pp. 281-284 (2015).

[4] H. R. Rossmann, U. Gysin, A. Bubendorf, T. Glatzel, S. Reshanov, A. Schöner, T. A. Jung, E. Meyer, H. Bartolf, "Two-Dimensional Carrier Profiling on Lightly Doped n-type 4H-SiC Epitaxially Grown Layers," Mat. Sci. For., Vols 821-823 (2015), pp 269-272.